Defence Technology 13 (2017) 6–15

Contents lists available at ScienceDirect

Defence Technology

journal homepage: www.elsevier.com/locate/dt

Trans-dinitroglycoluril isomers-A DFT treatment

Lemi Türker*

Middle East Technical University, Department of Chemistry, Ankara, Turkey

ARTICLE INFO

Article history:
Received 4 November 2016
Received in revised form
11 December 2016
Accepted 20 December 2016
Available online 30 December 2016

Keywords:
Trans-dinitroglycoluril
DINGU
Nitramines
DFT calculations
Protonation
Tautomerism

ABSTRACT

Isomers of *trans*-1,4-Dinitroglycoluril (*trans*-DINGU) and their 1,3-tautomers are considered within the constraints of B3LYP/6-31++G (d,p) and B3LYP/CC-PVTZ levels of DFT calculations. Additionally, the interactions of these isomers and proton in vacuum are investigated. The data have revealed that two of the three isomers undergo C–H bond cleavage as the result of interaction with proton in vacuum. The total energies, some structural properties, the calculated IR and UV spectra are discussed.

1. Introduction

The chemical, known as *cis*-1,4-Dinitroglycoluril (*cis*-DINGU) [1,2], is an important explosive and it has been of interest to the high energy materials community recently. *cis*-DINGU was prepared as early as 1888 by Franchimont and Klobbie [3,4]. Then various synthesis of *cis*-DINGU and its derivatives were described in the literature [5–9]. It has been fully characterized [2,10,11] Nowadays *cis*-DINGU is regarded as one of the potential ingredients for low vulnerability ammunition applications [12]. It has been as an insensitive alternative to RDX (hexahydro-1,3,5-trinitro-*s*-triazine) and TNT (trinitro-toluene) [13]. Table 1 displays some properties of *cis*-DINGU and some selected explosives.

Furthermore, *cis*-DINGU based PBXs (polymer bonded explosives) [15,16] generally have good physico-chemical stability, high explosion energy and low vulnerability, so that they are comparable to TATB (triamine-trinitro-bezene)-based PBXs. DINGU/Estane PBXs were investigated in detail [11]. Ternary compositions of *cis*-DINGU with TNT and RDX was the subject of a patent work [16].

The preparation of *cis*-DINGU is very simple and make use of inexpensive starting materials as compared to TATB. Therefore, *cis*-DINGU based PBXs have preference over TATB based PBXs [17]. Also toxicological studies on *cis*-DINGU were done [18] and the data have revealed that it would be considered only slightly toxic according to the classical guidelines. In the literature, there are many studies on *cis*-DINGU including its synthesis [5–7], structure determination (X-ray diffraction for *cis*-DINGU) [19], evaluation of the solid-state formation enthalpy [20], spectro-thermal decomposition [21], mass-spectral fragmentation pathways [22], modelization by molecular mechanics [23], modelization by using AM1 and PM3 methods [24]. In contrast to many reports on *cis*-DINGU, there is no study on *trans*-DINGU (*trans*-1,4-dinitroglycoluril) to the best of our knowledge (neither its synthesis nor X-ray crystallographic investigation) except a computational study exists where the performed DFT and *ab initio* calculations revealed some structural, quantum chemical and thermal properties of DINGU configurational isomers (*cis*- and *trans*- DINGU) in the gas phase [25]. In the present study, isomers of *trans*-1,4-Dinitroglycoluril (*trans*-DINGU) are considered within the constraints of B3LYP/6-31++G (d,p) and partly B3LYP/CC-PVTZ levels of DFT calculations.

2. Method

The initial geometry optimizations of all the structures leading to energy minima were achieved by using MM2 method followed by semi-empirical PM3 self-consistent fields molecular orbital (SCF MO) method [26,27] at the restricted level [28,29].

Subsequent optimizations were achieved at Hartree-Fock level using various basis sets. Then, geometry optimizations were

* Tel.: +90 3122103244.
E-mail address: lturker@metu.edu.tr.
Peer review under responsibility of China Ordnance Society.

http://dx.doi.org/10.1016/j.dt.2016.12.002

Table 1
Some properties of selected explosives.

	TNT	RDX	HMX	*cis*-DINGU
Oxygen balance/%	73.9	21.6	21.6	27.6
Density/(g·cm ^{3})	1.654	1.82	1.87 α form	1.94
			1.96 β	1.98 [11]
			1.82 γ	
			1.78 δ	
Energy of formation/(kJ·kg ^{1})	219.0	401.8	353.6	
Heat of formation/(kJ·kg ^{1})	295.3	301.4	253.3	42.3, 46/(kcal·mol ^{1}) [11]
Volume of explosion/(l·kg ^{1})	825	903	902	
Heat of explosion (H_2O gas)/(kJ·kg ^{1})	3646	5297	5249	
Velocity of detonation (confined)/(m·s ^{1})	6900	8750	9100	7580
	ρ:1.60/(g·cm ^{3})	ρ:1.76/(g·cm ^{3})	ρ:1.9/(g·cm ^{3})	ρ: 1.75/(g·cm ^{3})
Impact sensitivity/Nm	15	7.5	7.4	5–6
Friction sensitivity/N	353	120	120	20–300

Data excerpted from Ref. [14].

managed within the framework of density functional theory (DFT, B3LYP) [30,31] finally at the levels of 6–31++G (d,p) (restricted closed-shell) or CC-PVTZ [28,32]. The exchange term of B3LYP consists of hybrid Hartree–Fock and local spin density (LSD) exchange functions with Becke's gradient correlation to LSD exchange [31,33]. The correlation term of B3LYP consists of the Vosko, Wilk, Nusair (VWN3) local correlation functional [34] and Lee, Yang, Parr (LYP) correlation correction functional [35]. The vibrational analyses were also done. The total electronic energies are corrected for the zero point vibrational energy (ZPE). The normal mode analysis for each structure yielded no imaginary frequencies for the 3*N* 6 vibrational degrees of freedom, where *N* is the number of atoms in the system. This indicates that the structure of each molecule corresponds to at least a local minimum on the potential energy surface. All these calculations were done by using the Spartan 06 package program [36].

3. Results and discussion

A nitramine type explosive, known as simply DINGU, is constitutionally *cis*-1,4-dinitroglycoluril [25]. However, it should have also *trans* form which has not been synthesized yet. In addition to that either *cis* or *trans* forms of dinitroglycoluril should have other isomers which possess the nitramine group at different positions of the bicyclic system. In the present study, *trans*-dinitroglycoluril skeleton is considered in which three isomers exist arising from positional variations of the nitramine groups and they are indicated by capital letters as A,B and C.

3.1. Trans- dinitroglycoluril isomers

In the present study, three possible structural isomers of *trans*-dinitroglycoluril have been considered (Fig. 1). As seen in the figure, the *trans* forms of DINGU isomers possess bridge-head hydrogens oriented on opposite sites of the molecular plane, namely in the case of DINGU, *cis* and *trans* are defined with respect to the orientation of those hydrogens but not the nitro groups. The figure also shows the direction of the dipole moments they have. The isomers possess two nitramine groups which are anked by at least one pure amide carbonyl group arising from the particular structure of glicoluryl backbone. Fig. 2 shows the bond lengths and Table 2 contains their area, volume and dipole moment values. In structure-A the nitramine bond lengths are almost the same, C=O bonds comparable and the amide C–N bonds are symmetrically equal. Structure-B possesses unequal nitramine bond lengths, whereas in structure-C, they are comparable (see Fig. 2 for details). The dipole moments of these isomeric structures follow the order of B > A > C.

Inspection of the bond length data reveals that in structure-B, one of the nitramine bonds is longer (1.49 Å) than the others. It is the longest of all the nitramine bonds in structure-A through C. Also the carbonyl bond anked by that particular nitramine bond is longer (1.20 Å) than all the carbonyl bonds of these isomers. Based on classical resonance treatment, this fact could be explained if the nitramine, amine nitrogen lone-pair shifts towards the carbonyl group rather than to the nitro group. It might arise because of the geometrical factors operative in that particular ring, thus preventing the conjugation with the nitro group (see Figs. 1 and 2).

Table 3 shows the total energies (E), the zero point vibrational energies (ZPE) and the corrected total energies (E_c) which contain the ZPE values at the level of B3LYP/6-31++G (d,p). E_c value of DINGU (cis-1,4-dinitroglycoluril) is 2453243.40 kJ/mol. Thus, the stability order based on E_c values is DINGU > C > A > B. Note that isomer-B has the greatest dipole moment among the set and the dipole moment of isomer-C is zero. Aqueous energies are obtained based on SAM5.4 model of Cramer and Truhlar [37]. In water the stability order is C > B > A. It means solvation effects on A and B in aqueous medium reverses the stability order of them while C remains the most stable one as it is in vacuum. Table 4 shows the similar energies obtained at the level of B3LYP/CC-PVTZ. Note that CC-PVTZ is a correlation consistent basis set. The stability order based on E_c values in this case is again DINGU > C > A > B.

The stability orders in vacuum and water indicate that isomer-C where the nitramine groups are crossly located is more stable than the others. Isomer-A having two nitramine groups on the same ring is the least stable in water. Isomer-B, the least stable in vacuum is somewhat stabilized by solvation and becomes more stable than isomer-A.

Fig. 3 displays the IR-spectra of the isomers considered. The N–H stretchings occur around 3600 cm ^{1}. In the spectra of isomer-

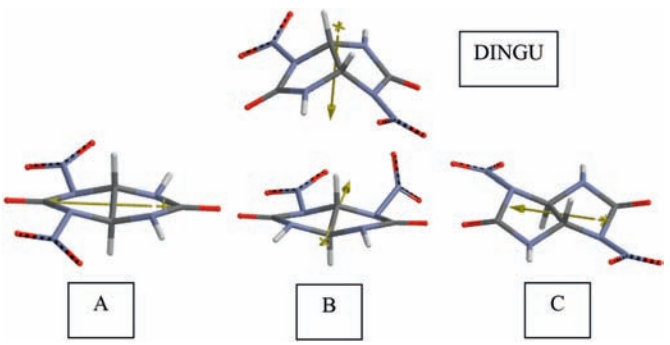

Fig. 1. *cis*-1,4-Dinitroglycoluril (DINGU) and isomers of *trans*-dinitroglycoluril (B3LYP/6-31++G (d,p) level of calculations).

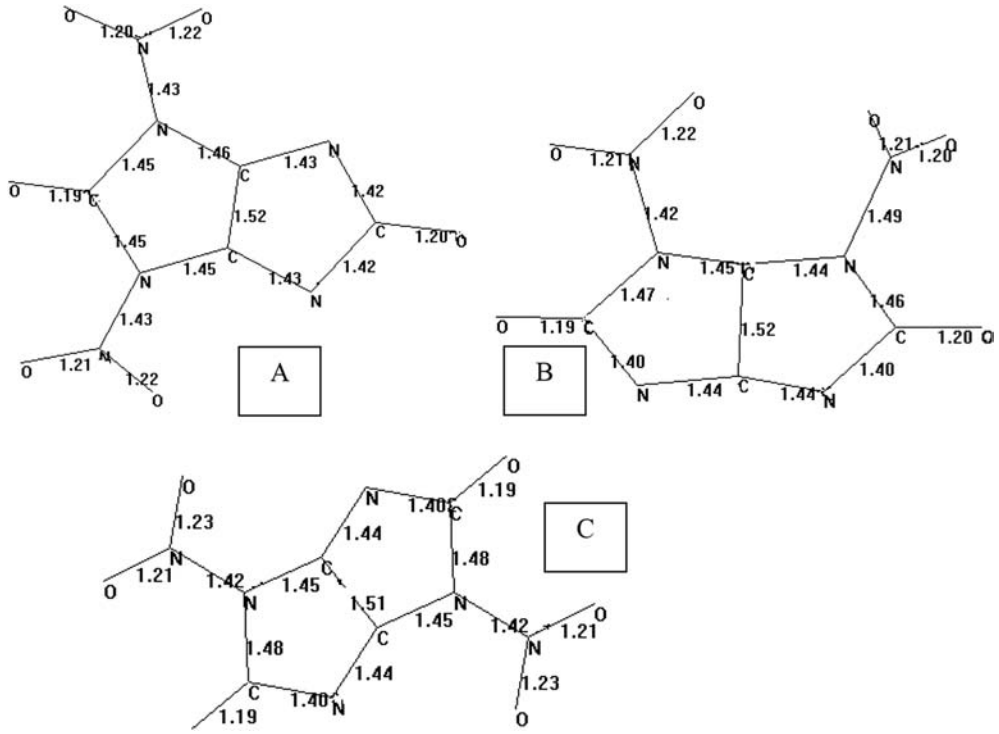

Fig. 2. Bond lengths (Å) in the isomeric structures considered (Hydrogens not shown, B3LYP/6-31++G (d,p) level of calculations).

Table 2
Some properties of the isomers considered.

	Area 10−20/m^2	Volume 10−30/m^3	Dipole moment/Debye
A	196.06	164.37	1.49
B	196.68	165.02	7.06
C	196.17	164.38	0.00

B3LYP/6-31++G(d,p) level of calculations. All the isomers possess C1 symmetry.

Table 3
Various energies of the isomers considered.

	E	*ZPE*	E_c	E_{aq} (corrected)
DINGU	2453573.85	330.45	2453243.40	2453268.21
A	2453455.65	331.21	2453124.44	2453140.82
B	2453429.48	329.82	2453099.66	2453142.64
C	2453465.60	331.33	2453134.27	2453157.00

Energies in kJ/mol. $E_c = E + ZPE$, B3LYP/6-31++G(d,p) level of calculations.

Table 4
Various energies of the isomers considered.

	E	*ZPE*	E_c
DINGU	2454377.75	330.26	2454047.49
A	2454259.73	330.70	2453929.03
B	2454233.25	329.24	2453904.01
C	2454269.07	330.89	2453938.18

Energies in kJ/mol. $E_c = E + ZPE$, B3LYP/CC-PVTZ level of calculations.

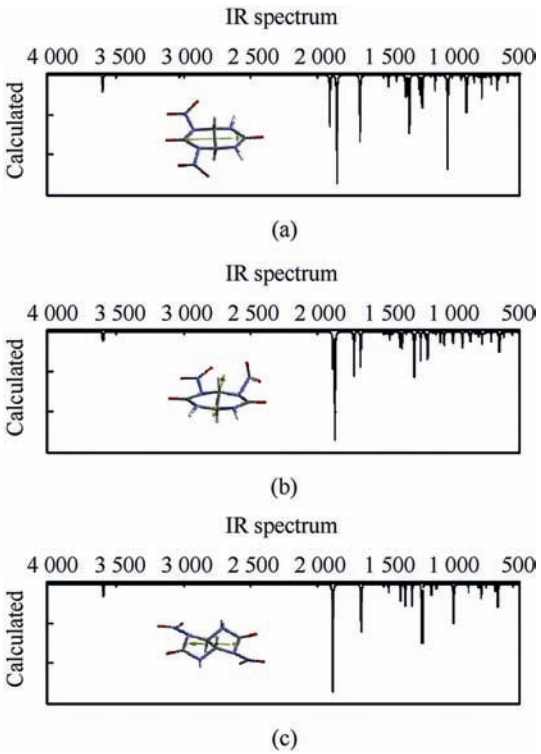

Fig. 3. IR spectra of the isomers (B3LYP/6-31++G (d,p) level of calculations).

A, the band at 1908 cm ^{1} is the stretching of C═O bond in the cycle having the nitro groups. The other carbonyl bond stretches at 1855 cm ^{1}. The bending of nitramine bonds coupled with N–O stretchings occurs at 1684 cm ^{1} and they are all strong. The twisting of the backbone occurs at 1317 cm ^{1}. In structure-B, carbonyl stretchings occur at 1886 and 1870 cm ^{1}. The bands at 1731 and 1680 stand for the bending of nitramine bonds coupled with N–O stretchings. The twisting of the backbone occurs at 1278 cm ^{1}. Structure-C has very strong C═O stretching at 1886 cm ^{1}. The next strong band is the bending of nitramine bonds

coupled with N–O stretchings and occurs at 1676 cm ^{1}.

Table 5 displays the selected experimental IR absorptions for *cis*-DINGU excerpted from the literature [10] and the presently calculated ones for *trans*-DINGU.

It has been reported that the IR spectra recorded as a function of time during the thermal decomposition reveals intensity loss for all the bonds as expected, but the IR spectra at 250 and 360 C and at 90 and 100 min are conspicuous for the near absence of NO_2 bands at 1570 and 1270 cm ^{1} and N–N band at 1180 cm ^{1}, with the retention of all other bands to a reasonable extend. This is direct evidence for the preferential N–NO_2 rupture as observed in similar systems [21].

Table 6 displays the frontier molecular orbital energies, namely the HOMO and LUMO energies and the interfrontier molecular orbital energy gaps ($\Delta\varepsilon$) which is the LUMO-HOMO energy difference. The HOMO energies (by the both level of calculations) follow the order of C < *cis*-DINGU < B < A, whereas the LUMO energies have the order of A < C<B< *cis*-DINGU. Consequently, $\Delta\varepsilon$ order becomes *cis*-DINGU > C > B > A (B3LYP/6-31++G (d,p)) but C> *cis*-DINGU > B > A (B3LYP/CC-PVTZ). Fig. 4 shows some of the molecular orbital energy levels of the isomers. The inner lying occupied molecular orbital energy levels show diversity.

It is known that the impact sensitivity of explosives increases as the HOMO-LUMO energy gap decreases [38]. So, isomer-A which possesses two nitramine groups embedded into the same ring is predicted to be more sensitive to impact than the others.

The time dependent DFT (B3LYP/6-31++G (d,p)) calculations showed that the UV-VIS spectra of the isomers exhibit rather simple pattern. The absorptions are confined to UV region only, below 375 nm for isomer-B and below 350 nm for structures A and C. Since, there is no extended conjugation spread over the whole backbone of these isomers, the structural variations arising from position of the nitramine moieties do not affect the UV-VIS spectra noticeably.

As seen in Fig. 5, in the case of isomer-A, the nitro groups do not contribute to the HOMO and the embedded urea moiety is the main contributor. Whereas in B and C, they contribute some but in different extent in the same molecule. In B the embedded amide moieties are the effective contributors of the HOMO. The contributions of the nitro groups in to the LUMO are appreciable in all the cases. As a result of these varying contributions the HOMO and LUMO energy levels (Table 6 and Fig. 4) differ somewhat from isomer to isomer.

3.2. Trans- dinitroglycoluril 1,3-tautomers

The type of breaking and forming of chemical bonds divides reactions into two categories; namely homolytic and heterolytic (radical and ionic, respectively). It may be postulated that tautomeric conversions of both types must exist. However, up to the present time mostly heterolytic (cationotropic and anionotropic) tautomeric conversions have been studied [39]. The isomers presently considered may exhibit tautomerism.

Table 6
Frontier molecular orbital energies and interfrontier molecular orbital energy gaps ($\Delta\varepsilon$) of the isomers considered.

	B3LYP/6-31++G (d,p) level			B3LYP/CC-PVTZ level		
	HOMO	LUMO	$\Delta\varepsilon$	HOMO	LUMO	$\Delta\varepsilon$
Cis-DINGU	847.96	290.14	557.83	830.72	255.98	574.74
A	826.38	327.66	498.72	810.76	293.03	517.73
B	840.68	296.84	543.83	824.75	259.74	565.01
C (*trans*-DINGU)	859.74	302.63	557.12	842.95	266.66	576.29

Energies in kJ/mol.

Fig. 6 shows the 1,3-tautomers (proton tautomerism) of the isomers considered. Note that in the case of B and C, doubly 1,3-tautomeric structures are possible. The tautomers are indicated as primed and doubly primed letters (for the doubly tautomeric structures).

Table 7 shows some properties of those tautomers. Note that B″ has the smallest area and volume. The order of dipole moments is C''<B''<C'<A'<B'. It should be because of the charge distribution and bond length variations from tautomer to tautomer. Note that vectorial sum of the bond dipoles dictate the resultant dipole moment of structures. However, the dipole moments of structures having double 1,3-tautomerism are less than their counterparts with single 1,3-tautomerism. This effect could be attributed to arising higher symmetry because of the double tautomerism.

Table 8 shows the total energies, ZPE values and the corrected total energies of the tautomers in vacuum and aqueous conditions. The data reveal that in vacuum the stability order is C'>A'>B'>C''>B″ and in water it is C'>B'>A'>C''>B''. The orders are almost the same except in water where A′ and B′ have exchanged their positions in the order. However, the energy difference between A′ and B′ in water is much less than the respective value in vacuum. The isomers and the 1,3-tautomers of them can be compared in terms of energy (they are all isomeric structures). Using the data in Tables 3, 4 and 8, one observes that the tautomers are less stable than their parent structures in vacuum as well as in water. Also note that doubly tautomeric structures B″ and C″ are less stable than their mono tautomeric counterparts.

Table 9 includes the HOMO, LUMO energies and $\Delta\varepsilon$ values for the tautomers. Tautomers C′ and C″ are characterized with the lowest and highest HOMO energy levels, respectively. As for the LUMO energies B″ and C″ are the ones having the lowest and highest levels, respectively. The order of $\Delta\varepsilon$ values is B''<A'<C''<B'<C'. As a consequence of this order, UV-VIS spectrum of B″ spans up to 400 nm which means the HOMO-LUMO excitation is much easier than the others. Accordingly, as mentioned above in

Table 5
Selected IR absorptions.

Cis-DINGU Experiment [10]	*trans*-DINGU (calculation level B3LYP/6-31++G (d,p))	*trans*-DINGU (calculation level B3LYP/CC-PVTZ)	Assignment
3388 s	3645 s	3590 s	NH
3245 b, w	3643 s	3590 w	NH
3178 w			NH
3006 w	3128 vw	3022 w	CH
2863 vw	3123 vw	3010 vw	CH
1810 s	1886 s	1894 vw	C=O
1772 vs	1874 vs	1886 vs	C=O
1570 s	1658 s	1665 s	NO_2
1565 s	1653 s	1663 vw	NO_2

w = weak, vw = very weak, s = strong, vs = very strong, m = medium. b = broad.

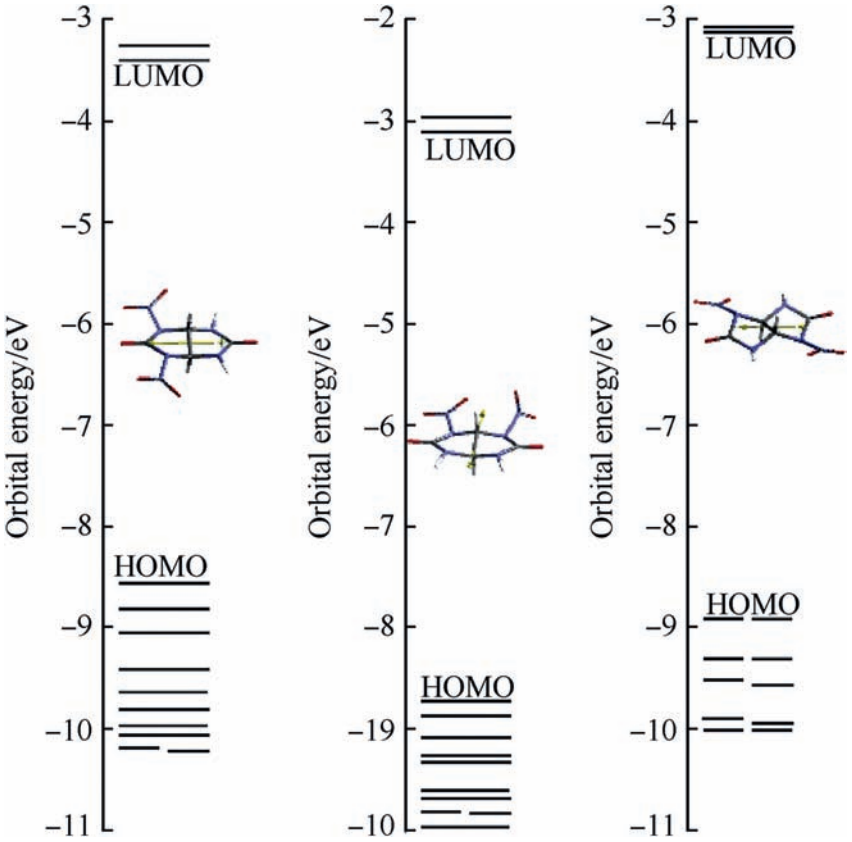

Fig. 4. Some of the molecular orbital energy levels of the isomers considered (B3LYP/6-31++G (d,p) level of calculations).

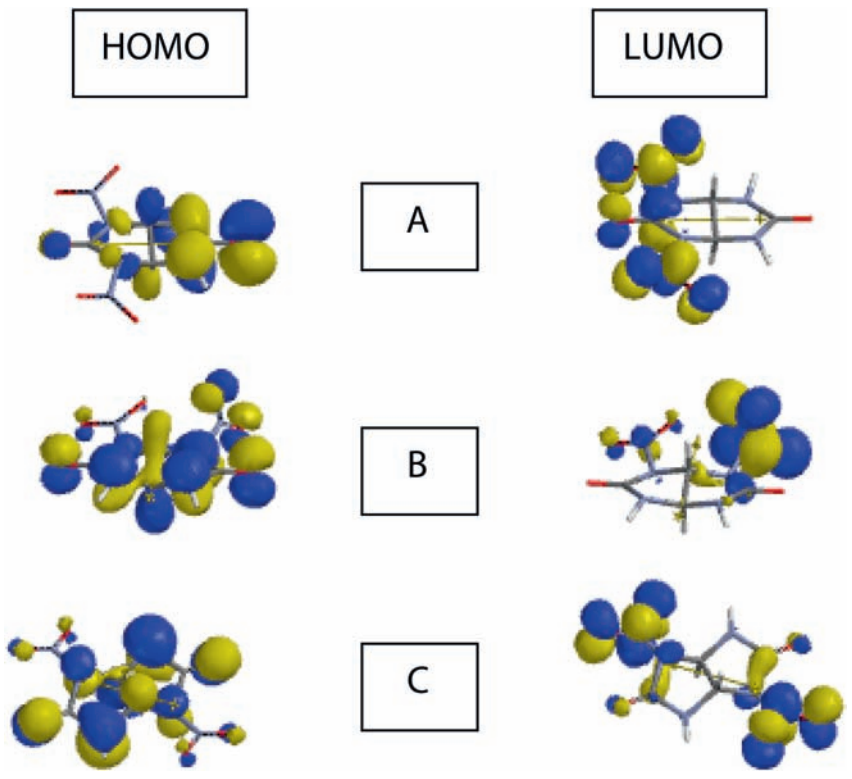

Fig. 5. The HOMO and LUMO pattern of the isomers considered (B3LYP/6-31++G (d,p) level of calculations).

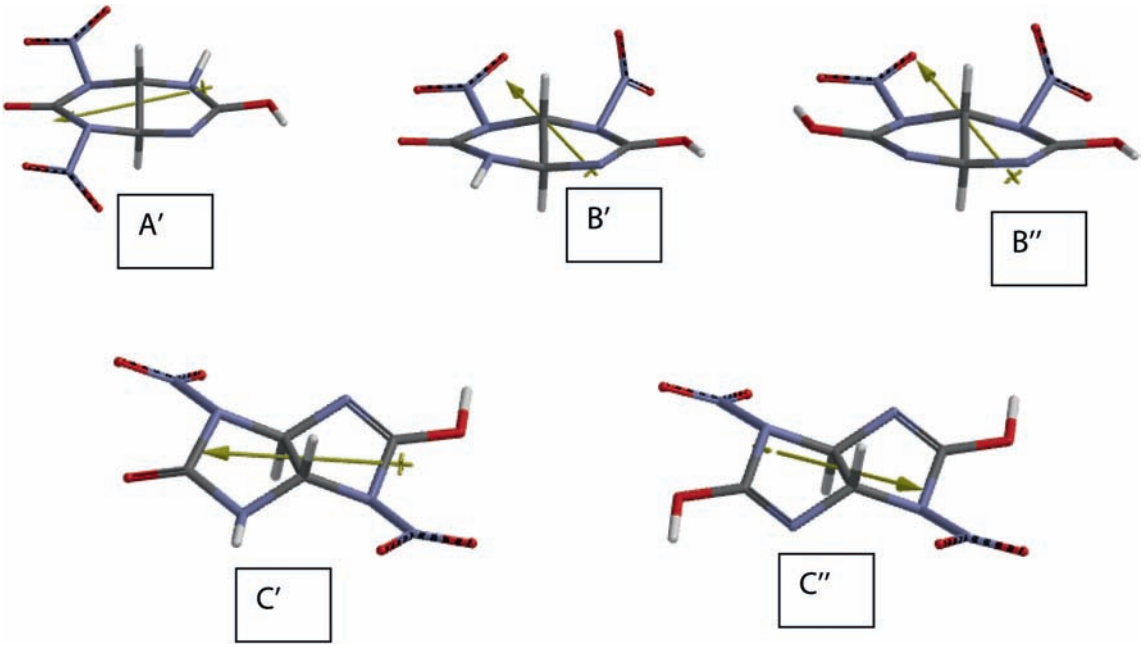

Fig. 6. 1,3-Tautomers of the isomers considered (B3LYP/6-31++G (d,p) level of calculations).

Table 7
Some properties of the tautomers considered.

	Area 10 ^{20}/m^2	Volume 10 ^{30}/m^3	Dipole moment/Debye
A'	196.02	164.07	5.73
B'	196.99	164.67	6.47
B''	192.67	163.37	1.68
C'	195.79	164.11	3.85
C''	195.37	163.83	0.00

B3LYP/6-31++G(d,p) level of calculations. All the isomers possess C1 symmetry.

Table 8
Various energies of the tautomers presently considered.

	E	*ZPE*	E_c	E_{aq} (corrected)
A'	2453379.08	329.88	2453049.20	2453096.31
B'	2453366.40	328.60	2453037.80	2453099.72
B''	2453304.70	327.23	2452977.47	2453035.85
C'	2453384.87	330.00	2453054.87	2453105.83
C''	2453306.21	328.46	2452977.75	2453052.13

Energies in kJ/mol. $E_c = E + ZPE$, B3LYP/6-31++G(d,p) level of calculations.

Table 9
Frontier molecular orbital energies and interfrontier molecular orbital gaps ($\Delta\varepsilon$) of the tautomers considered.

	HOMO	LUMO	$\Delta\varepsilon$
A'	772.97	302.13	470.84
B'	807.16	305.60	501.56
B''	772.80	326.30	446.50
C'	823.62	308.38	515.24
C''	771.64	271.52	500.12

Energies in kJ/mol. $E_c = E + ZPE$, B3LYP/6-31++G(d,p) level of calculations.

the light of reference [38], B″ should be more sensitive to impact than the other tautomers, even more sensitive than the parent structures (see Tables 6 and 9). However, B″ is the least stable tautomer in the group, hence its concentration in the tautomeric mixture should be low. Note that tautomers exist in the bulk in varying percentages dictated by their stabilities. Sometimes a tautomer having a small concentration might be more sensitive to certain stimuli than the others.

In the IR spectrum, tautomers A′,B′ and C′ have O–H stretching occurring at 3785, 3783, 3765 cm ^{1}, respectively. The N–H stretchings appear at 3581, 3600, 3598 cm ^{1}, whereas the carbonyl stretchings occur at 1902 cm ^{1},1884 cm ^{1}, 1882 cm ^{1}, respectively. In tautomer B″, O–H stretchings are at 3781 cm ^{1} and 3483 cm ^{1}, whereas in C″ it occurs at 3764 cm ^{1}. Obviously, B″ and C″ do not have any N–H and C=O bonds.

3.3. Protonated trans-dinitroglycoluril isomers

Protonation behavior of the isomers of *trans*-dinitroglycoluril have been considered as well in the present treatise. Only the mono protonation at the nitrogen and oxygen atoms of the same amide group have been considered. The N-protonated isomers are designated as AhN, BhN and ChN and O-protonated (amide oxygen of the same ring) ones as AhO, BhO and ChO. Their optimized geometries are shown in Fig. 7. Table 10 displays some energies of the mono protonated isomers. Stabilities based on the corrected total energy values in vacuum and water are the same, namely AhN > ChN > BhN for the N-protonated and ChO > AhO > BhO for the O-protonated forms. Note that the protonation in these isomers prevents delocalization of the lone-pair of nitrogen towards the carbonyl group. Only in the other ring, the amide nitrogen (if it exists) can supply electrons towards the carbonyl group. Hence, the solvation effects should, in great extent, operate in parallel for all these three species, yielding the same order of stabilities in vacuum and water.

Fig. 8 shows the IR spectra of the N-protonated isomers. In all the cases three distinct N–H peaks are observed in the calculated spectra. In isomer-A unprotonated N–H stretching occurs at 3562 cm ^{1}, whereas NH_2^+ (protonation site) asymmetric and symmetric stretchings happen at 3482 cm ^{1}and 3399 cm ^{1}, respectively. Two carbonyl peaks exist at 2026 cm ^{1} and 1944 cm ^{1}, where the former one stands for the carbonyl nearby the protonation site. In the case of isomer-B, N–H vibrations occur at

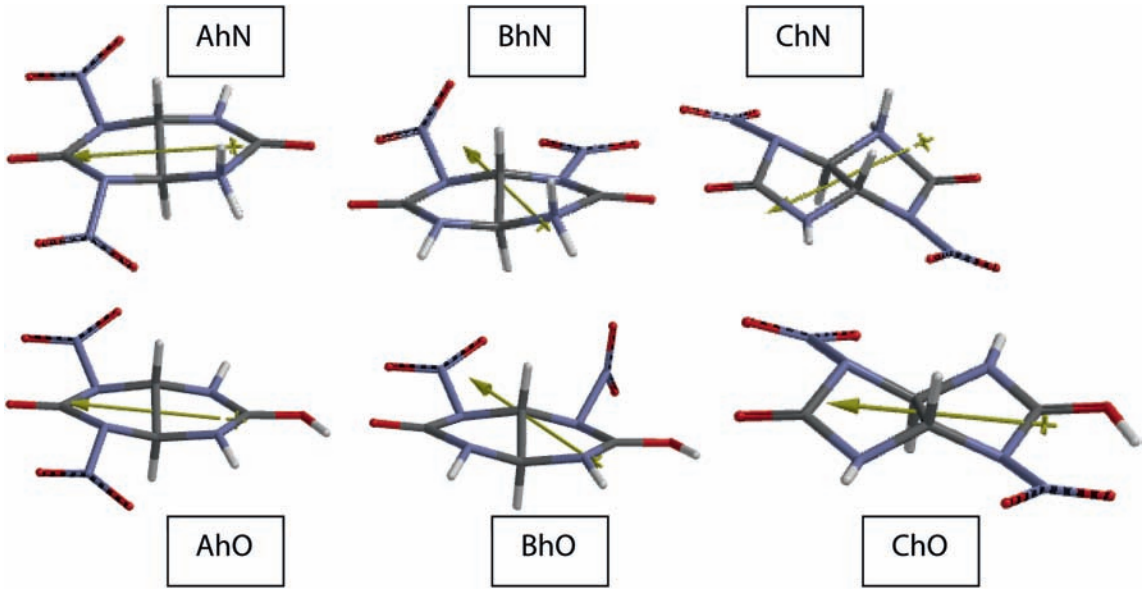

Fig. 7. Optimized structures of the protonated isomers (B3LYP/6-31++G (d,p) level of calculations).

Table 10
Some energies of the protonated isomers.

	E	*ZPE*	E_c	$E_{aq\ corr}$
AhN	2454241.98	361.83	2453880.15	2454144.79
BhN	2454193.40	359.47	2453833.93	2454101.88
ChN	2454222.11	361.88	2453860.23	2454124.85
AhO	2454269.60	362.01	2453907.59	2454269.60
BhO	2454217.19	359.35	2453857.84	2454217.19
ChO	2454273.13	362.55	2453910.58	2454273.13

Energies in kJ/mol. $E_c = E + ZPE$, B3LYP/6-31++G(d,p) level of calculations.

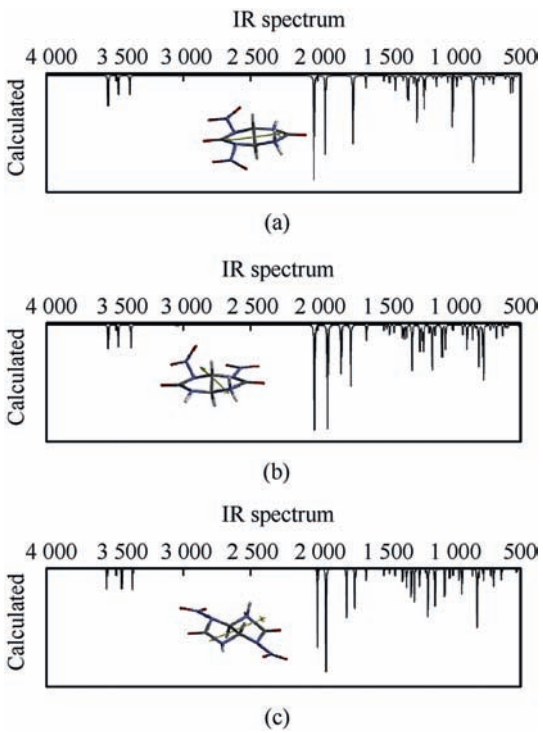

Fig. 8. IR spectra of the N-protonated isomers (B3LYP/6-31++G (d,p) level of calculations).

3567 cm ^{1}, 3490 cm ^{1} and 3395 cm ^{1} where the last two are asymmetric and symmetric stretching of the NH_2^+ group, respectively. The C═O vibrations occur at 2024 cm ^{1} (which is nearby the NH_2^+) and 1926 cm ^{1}. In isomer-C, the N–H vibrations are at 3578 cm ^{1} (N–H), 3464 cm ^{1} (asym.NH_2^+) and 3384 cm ^{1} (sym NH_2^+), whereas the carbonyl stretchings occur at 2001 cm ^{1} (C═O nearby NH_2^+) and 1937 cm ^{1} (C═O). The O-protonated species AhO and BhO have two peaks around 3500 cm ^{1}. The O–H stretchings in AhO, BhO and ChO occur at 3748 cm ^{1}, 3754 cm ^{1} and 3421 cm ^{1}, respectively. The N–H stretchings appear at 3571 cm ^{1}, 3574 cm ^{1}, for AhO and BhO, respectively and 3579 cm ^{1} and 3554 cm ^{1} for ChO. The carbonyl C═O peaks happen at 1943 cm ^{1} and 1680 cm ^{1}; 1926 cm ^{1} and 1649 cm ^{1}; 1933 cm ^{1}and 1678 cm ^{1}, respectively for AhO, BhO and ChO. The lower bands stand for amide CO where the protonation occurred.

In all the three N-protonated species, one of the amide nitrogens has been blocked. Besides, the inductive effect of NH_2^+ group makes C═O bond to have more double bond character in its resonance forms. Thus, C═O group adjacent to the protonation site vibrates at higher values compared to the stretching of the other carbonyl group which has an amide group (structures BhN and ChN). Structure-AhN does not have pure amide moiety in the unprotonated ring (two nitramine groups exist) and its C═O stretchings have the highest values (2026 cm ^{1} and 1944 cm ^{1}) compared to the other N-protonated structures.

All the protonated isomers absorb in the UV region only. Table 11 shows the frontier molecular orbital energies and the interfrontier energy gaps. The Δε order is

Table 11
Frontier molecular orbital energies and interfrontier molecular orbital energy gaps (Δε) of the protonated isomers considered.

	HOMO	LUMO	Δε
AhN	1257.29	671.07	586.22
BhN	1218.44	707.59	510.85
ChN	1232.39	725.10	507.29
AhO	1228.01	639.13	588.88
BhO	1188.67	696.25	492.43
ChO	1211.15	779.81	431.34

Energies in kJ/mol. B3LYP/6-31++G(d,p) level of calculations.

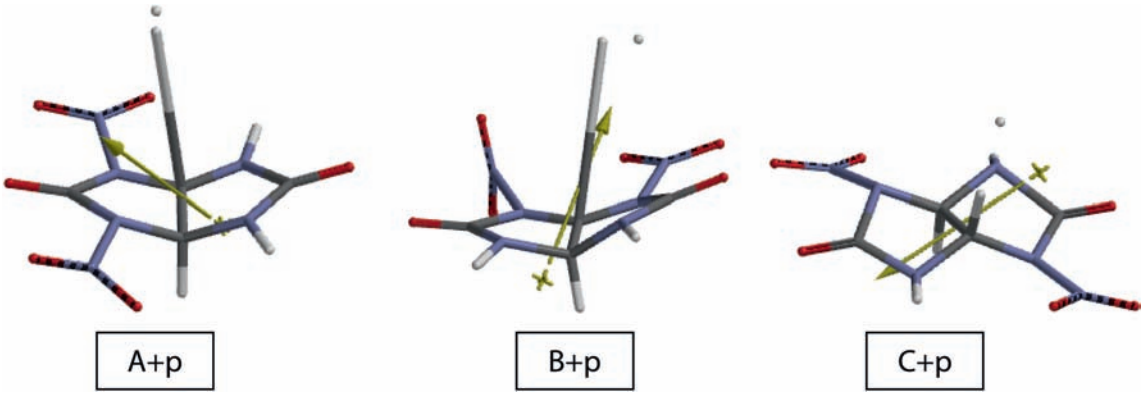

Fig. 9. Optimized structures of the composite systems considered (B3LYP/6-31++G (d,p) level of calculations).

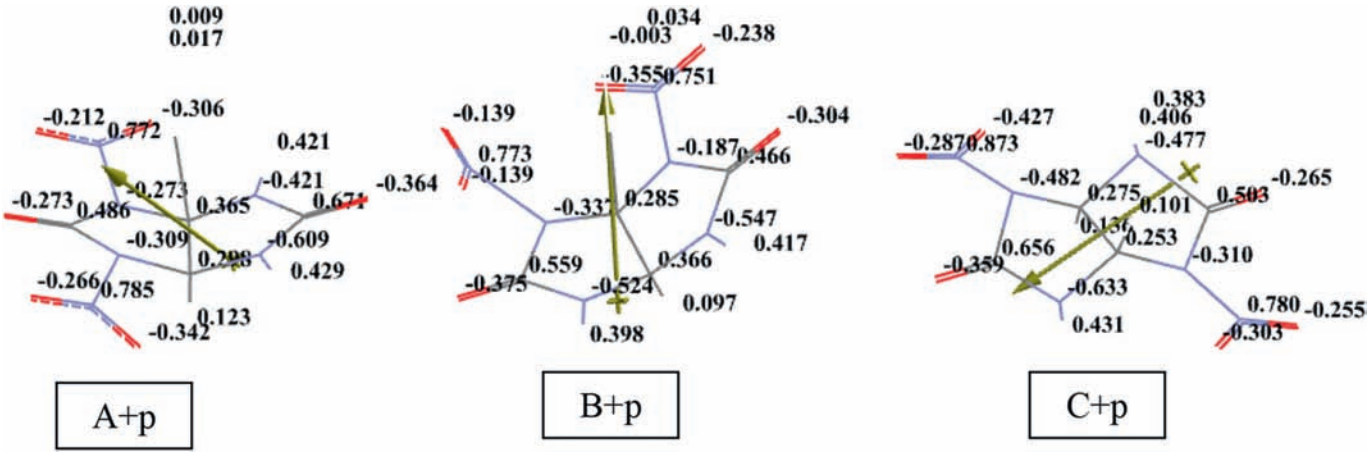

Fig. 10. Electrostatic charge distribution in the composite systems (B3LYP/6-31++G (d,p) level of calculations).

AhO > AhN > BhN > ChN > BhO > ChO and the UV spectra have the λ_{max} values in accord with reverse order of this of $\Delta\varepsilon$ sequence.

3.4. Effect of proton on trans-dinitroglycoluril isomers in vacuum

The most interesting feature of *trans*-dinitroglycoluril isomers arises when they are subjected to effect of proton in vacuum. This condition could be achieved either in laboratory or attained in interstellar space where protons available in cosmic rays [40]. The presently considered isomers and proton are considered as composite systems (eg., A + p). In the present model, the proton is considered to be static. Figs. 9 and 10 show the optimized structures and electrostatic charge distribution of the composite systems, respectively. Although, in the case of isomers A and B the C–H bond at the bridgehead position is broken, isomer-C is stable (some small bond length changes occur only). As a conjecture cis-DINGU should exhibit such kind of behavior too. The distances between the H and C atoms of the broken bond at the bridgehead position are 3.56 Å and 3.58 Å in isomer-A and –B, respectively (Fig. 11). The data in Fig. 10 indicate that the nearby proton has highly lost its positive charge.

In composites A + p and B + p the hydrogen-hydrogen distances are both 0.745 Å which are both suitable bonding distance of H_2 molecule (0.744 Å calculated at the same level of DFT). In isomer-C hydrogen-hydrogen distance is 1.66 Å and C–H bond at the site of consideration is 1.02 Å.

Table 12 tabulates various energies of the composite systems considered. Inspection of the E_c values reveals that the stability order follows the sequence of A + p > C + p > B + p. Note that the electrostatic field of the nearby proton perturbs the electrostatic field of the molecule and the stability order of isomers (C > A > B) changes great deal. Note that the stability order considered above is the overall stability of the composite system not the heterocyclic part alone.

In the calculated IR spectrum of A + p system the N–H stretchings occur at 3602 cm ^{1} and 3559 cm ^{1}. Whereas the carbonyl stretchings happen at 1966 cm ^{1} and 1951 cm ^{1}. In composite B + p system, the peaks at 3604 cm ^{1}and 3595 cm ^{1} stand for the N–H stretchings and the C=O stretchings appear at 1961 and 1909 cm ^{1}. In C + p composite three distinct N–H peaks are observed (3580, 3466 and 3387 cm ^{1}) and the carbonyl stretchings occur at 2001 cm ^{1} and 1936 cm ^{1}.

Table 13 shows the frontier molecular orbital energies and interfrontier molecular orbital energy gaps ($\Delta\varepsilon$) of the composite systems considered. The $\Delta\varepsilon$ order is C + p > A + p > B + p. Following this order reversely, the UV spectrum of B + p occurs in the range of 200–400 nm while the others span in between 200 and 350 nm.

Note that the HOMO and LUMO energies follow the order of C + p > B + p > A + p whereas for the isomers the HOMO energy order is C < B < A and the LUMO order is B > C > A. So the presence of the proton in the composite systems most effectively lowers the HOMO of A than B and C.

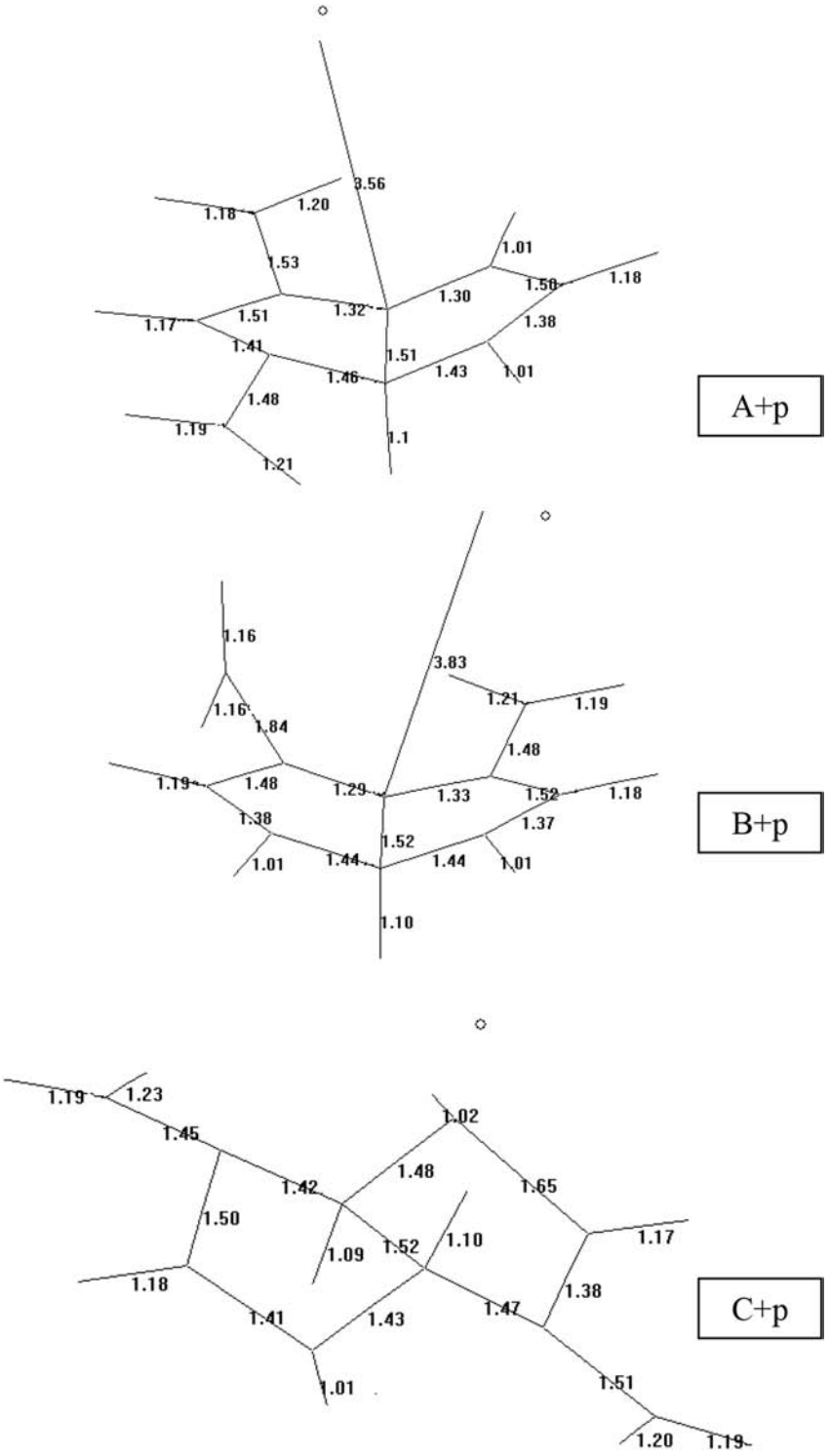

Fig. 11. Bond lengths and distances (Å) in the composite systems (B3LYP/6-31++G (d,p) level of calculations).

Table 12
Various energies of the composite systems (isomers and proton) considered.

	E	*ZPE*	E_c
A + p	2454205.4	325.75	2453879.65
B + p	2454164.55	322.94	2453841.61
C + p	2454222.11	361.82	2453860.29

Energies in kJ/mol. . $E_c = E + ZPE$, B3LYP/6-31++G(d,p) level of calculations.

Table 13
Frontier molecular orbital energies and interfrontier molecular orbital energy gaps ($\Delta\varepsilon$) of the composite systems considered.

	HOMO	LUMO	$\Delta\varepsilon$
A + p	1297.86	803.38	494.48
B + p	1247.9	800.8	447.1
C + p	1232.38	725.31	507.07

Energies in kJ/mol. B3LYP/6-31++G(d,p) level of calculations.

4. Conclusion

Within the constraints of level of calculations performed presently, *trans*-dinitroglycoluril isomers exhibit highly structure-dependent properties that is the location of the nitramine group dictates various geometrical, physical and quantum chemical properties. Both in the vacuum and water the isomer having the nitramine groups farthest away from each other (isomer-C) is the most stable one. It is also true for the 1,3-tautomers considered. As for the protonated isomers, O-protonated ones are overall more stable than their N-protonated isomers and also the former ones are more stable than their respective N-protonated counterparts. The interaction of the isomers with proton in vacuum causes tertiary C–H bond to cleave from relatively less stable isomers, A and B, but the most stable isomers (C) remains intact.

All these results might provide some insight for researchers interested in *trans*-dinitroglycoluril isomers.

References

[1] Boileau J, Carail M, Wimmer E, Gallo R, Pierrot M. Propell Explos Pyrotech 1985;10:118–20.
[2] Boıleau J, Wımmer E. Acta Cryst 1988;C44:696–9.
[3] Franchimont APN, Klobbie EA. Recl Trav Chim 1888;7:343–8.
[4] Franchimont APN, Klobbie EA. Recl Trav Chim 1889;8:283–92.
[5] Boileau J, Wimmer E, Carail M, Gallo R. Bull la Soc Chim Fr 1986;3:465–9.
[6] Boileau J, Wimmer E, Carail M, Gallo R. Propell Explos Pyrotech 1985;10:118–20.
[7] Boileau J, Emeury M, De Longueville Y, Monteagudo P. Chem Mech Technol Treib- Explos 1981:505–26.
[8] Zharkov MN, Kuchurov IV, Fomenkov IV. Zlotin SGi Tartakovsky VA. Mendeleev Commun 2015;25:15–6.
[9] Sherrill WM, Johnson EC, Paraskos AJ. Propellants explos. Pyrotech 2014;39:90–4.
[10] Oyumi Y, Brill TB. Propellants, explosives. Pyrotechnics 1988;13:69–73.
[11] Stinecipher MM, Stretz LA. Los Alamos National Laboratory LA-UR–85-139O DE85 010750.1985.
[12] Jiamin L. Proceedings of the Seventeenth International Pyrotechnich Seminar Combined with Second Beijing International Symposium on Pyrotechnics and Explosives, vol. 1, Beijing, 1992; 322–332.
[13] Agrawal JP. Prog Energy Combust 1998;24:1–30.
[14] Meyer R, Köhler J, Homburg A. Explosives. Weinheim: Wiley-VCH; 2002.
[15] Chovancova M, Zeman S. Thermochim Acta 2007;460:67–76.
[16] Kehren JPA, Ousset RA. US 4,148,674. Apr. 10, 1979.
[17] Sikder AK, Sikder N. J Hazard Mater A 2004;112:1–15.
[18] London JE, Smith DM. Avail NTIS Rep 1984;9(14). Absract no. 26903.
[19] Boileau J, Wimmer E, Gilardi R, Stinecipher MM, Galio R, Pierrot M. Acta Crystallogr 1988;44:696–9.
[20] Mathieu D, Simonetti P. Thermochim Acta 2002;384:369–75.
[21] Khire VH, Talawar MB, Prabhakaran KV, Mukundan T, Kurian EM. J Hazard Mater A 2005;119:63–8.
[22] Yinon J, Bulusu S, Axenrod T. Org Mass Spectrom 1994;29:625–31.
[23] Delpeyroux D, Blaive B, Gallo R, Graindorge H, Lescop L. Propell Explos Pyrotech 1994;19:70–5.
[24] Paz D, Luis J, Ciller GJ. Propell Explos Pyrotech 1993;18:33–40.
[25] Türker L, Atalar T. J Hazard Mater A 2006;137:47–56.
[26] Stewart JJP. J Comput Chem 1989;10:209–20.
[27] Stewart JJP. J Comput Chem 1989;10:221–64.
[28] Leach AR. Molecular modeling. Essex. Longman; 1997.
[29] Fletcher P. Practical methods of optimization. New York: Wiley; 1990.
[30] Kohn W, Sham L. J Phys Rev 1965;140:1133–8.
[31] Parr RG, Yang W. Density functional theory of atoms and molecules. London: Oxford University Press; 1989.
[32] Cramer CJ. Essentials of computational chemistry. Chichester, West Sussex: Wiley; 2004.
[33] Becke AD. Phys Rev A 1988;38:3098–100.
[34] Vosko SH, Vilk L, Nusair M. Can J Phys 1980;58:1200–11.
[35] Lee C, Yang W, Parr RG. Phys Rev B 1988;37:785–9.
[36] SPARTAN 06. Irvine CA, USA: Wavefunction Inc; 2006.
[37] Chambers CC, Hawkins GD, Cramer CJ, Truhlar DG. J Phys Chem 1996;100:16385–98.
[38] Ovens EJ. J Mol Struct (Theochem) 1984;121:213–20.
[39] Reutov O. Theoretical principles of organic chemistry. Moscow: Mir Pub; 1970.
[40] Friedlander G, Kennedy JW, Miller JM. Nuclear and radiochemistry. New York: Wiley; 1964.